PHYSICAL REVIEW B VOLUME 27, NUMBER 3 1 FEBRUARY 1983

Superconductivity of networks. A percolation approach to the effects of disorder

S. Alexander
The Racah Institute of Physics, The Hebrew University, Jerusalem 91904
and Department of Physics, University of California, Los Angeles, Los Angeles, California 90024
(Received 19 March 1982)

Solutions of the linearized Landau-Ginzburg equations on networks of thin wires are studied. We derive linear-difference equations for the value of the order parameter at the junctions of the net with the use of the explicit form of the solutions on the wires. The technique is shown to be applicable to the diffusion equation, to harmonic lattice vibrations, and to the Schrödinger equation and results in equations similar to tight-binding equations. The equations are solved and the upper critical field is determined for some simple finite nets, for the infinite square net, and for the triangular Sierpinski gasket. Dead-end side branches are shown to lead to a mass renormalization. On the square net the equations map on the Azbel-Hofstadter-Aubry model. When the coherence length is small, vortex cores can be accommodated in the holes of the net and there is no upper critical field. The equations on the Sierpinski gasket are solved by an iterative decimation process. The process determines a new length scale proportional to a power of the bare coherence length. The upper critical field is studied for a finite gasket and for a lattice of gaskets. With the use of scaling arguments the results are applied to percolation clusters. Far from the percolation threshold the results are described by a renormalized correlation length of standard form. When this length becomes shorter than the correlation length for the percolation problem the critical field is shown to be constant or decreasing as the threshold is approached. Existing experiments are discussed and the importance of high-field-susceptibility measurements is emphasized.

I. INTRODUCTION

The purpose of this paper is to obtain a better understanding of the properties of disordered superconductors. We do this by studying behavior near the upper critical field. The motivation for this is twofold.

Deutscher *et al.*[1(a)] have recently studied the (zero-temperature) upper critical field of well-controlled, high-resistivity granular samples for which the resistivity is described by a percolation model.[1(b)] Far from the threshold the results are explained by relating the coherence length to the resistivity in the usual way. They also find a crossover to a new strongly disordered regime in which H_{c2} still increases with the resistivity, but the indices are different. They suggest that the crossover is due to the fact that the renormalized coherence length for superconductivity becomes comparable to the connectivity length of the underlying network.

From a theoretical point of view the study of upper critical fields has proven very useful in the past. One studies a ground-state property and thus avoids many of the difficulties associated with thermal fluctuations. Such a study should also yield information on the role of the anomalous short-distance properties of random systems in determining macroscopic behavior.

In two recent papers[2,3] de Gennes has studied related problems. He considers solutions of the linearized Landau-Ginzburg equations on nets of interconnected thin wires. de Gennes solves these equations on a loop with a dead-end side branch[22] and suggests an expression for the magnetic susceptibility of a finite cluster in terms of the loop distribution.[3] The validity of the approximation in Refs. 1 and 3 is not obvious and in any case one would like to have a systematic approach to random superconductors, which seem to show strange weak-link behavior.[4]

We follow Deutscher *et al.*[1] and de Gennes[2] and consider a purely geometric percolation model for the disorder. We therefore consider de Gennes's model of a network of thin superconducting wires.[3] We first develop a formalism, related to standard electric network technique, which allows us to solve the linearized Landau-Ginzburg equations on complex nets and to study their behavior under real-space renormalization transformations. This allows us to study the role of dead ends and subsidiary loops explicitly. Most of the paper is devoted to a study of specific finite and infinite nets.

The results confirm the relationship to the diffusion constant as long as the renormalized coherence length is large. The most interesting results relate to the strongly disordered regime. There are no consistent solutions of the linearized Landau-Ginzburg equations in this regime. Thus superconducting coherence disappears while the local amplitude of the order parameter remains finite. The characteristic length for superconducting correlations becomes shorter than the connectivity length of the net and is determined by the anomalous short-distance properties. It is related to the square of the bare superconducting coherence length by the same critical indices which relate the diffusion length to the diffusion time. It is found that the coherence length in this regime cannot be interpreted as a renormalized Landau-Ginzburg coherence length in the usual sense even at $T=0$. When combined with geometrical considerations it gives rise to a weak-link behavior in the strongly disordered regime.

The presence of a hierarchy of loops is crucial in determining the behavior in high magnetic fields. When such a hierarchy is present one predicts a weak-link behavior and a gradual breaking up of superconducting clusters containing smaller loops. If there are no subsidiary loops, flux quantization dominates and superconducting coherence cannot be destroyed by magnetic fields. The nonlinear coupling of amplitude and phase are crucial in describing this regime, which is quite different from the low-field situation considered in Ref. 3.

We believe the main features of our results reflect the anomalous short-distance behavior of the conductance and would show up also in a situation where localization is dominant. In Sec. II we derive our basic equations. We solve the linearized Landau-Ginzburg equations on the strands of a net using the (complex) junction amplitudes as boundary conditions. The solutions can then be used to express the matching conditions at the junctions[2,19] in terms of these amplitudes. One ends up with a set of linear equations, similar to electric network equations, which are easy to handle. We also discuss the generalization to the inhomogeneous linearized equations and their relationship to the nonlinear Landau-Ginzburg equations.

In Sec. III we discuss the relationship between the equations we derived and those arising in a number of other problems. We show the close relationship to the master equation for a diffusion problem, to electric network equations, and to the Schrödinger equation on the same net.

In Sec. IV we solve the equations for some finite nets. We demonstrate the renormalization of the coherence length for a line with dead-end side branches and for a ring with such branches. We also consider the behavior of two coupled loops.

In Sec. V we consider a square lattice. Like the equivalent electronic problem the equations map on a one-dimensional tight-binding problem with an incommensurate potential.[5-10] We show that the critical field (H_{c2}) is essentially equal to the bulk critical field as long as the Landau-Ginzburg coherence length (ξ_s) is large compared to the lattice spacing (a). Beyond a critical value of the ratio (ξ_s/a) of order 1, the net cannot be driven normal by a magnetic field. This reflects the fact that integral numbers of flux quanta through each loop can have no effect, leading to Little-Parks oscillations.[11]

In Sec. VI we consider solutions on a planar Sierpinski gasket. These gaskets have been studied by Gefen *et al.*[12] (GAMK) as a model for the percolation backbone. They have the interesting properties that they are self-similar under scale transformations and have anomalous dimensions and a hierarchy of loops. We use an iterative renormalization procedure, which is in principle exact, to solve the equations. We study the critical-field conditions for a finite gasket and for a lattice of equal finite gaskets. In a magnetic field an infinite gasket shows weak-link behavior. Large loops breakup gradually as the field is increased. It is finally driven normal at a field determined by the intrinsic coherence length on the gasket (H_s). For a lattice of gaskets we find a crossover when the intrinsic coherence length (λ) becomes comparable to the lattice spacing. For larger lattice spacings the critical field H_{c2} is larger than the field corresponding to flux quantization and smaller than the intrinsic critical field of the gasket (H_s). It decreases as the lattice spacing is increased. We interpret this as a weak-link behavior and suggest a scaling form.

In Sec. VII we analyze the Skal—Shklovskii—de Gennes[13] (SSG) model for percolation which has dead ends but no loops on a scale small compared to ξ_p. Using scaling ideas developed elsewhere[14] we relate the local coherence length to the anomalous diffusion length and determine the relevant indices. We find that this model cannot be driven normal by a field, beyond the crossover. This is an effect of flux quantization.

In Sec. VIII we discuss the results and compare them with the experimental results of Ref. 1. The weakly disordered regime is nicely described by our formalism and is not sensitive to the detailed model.

For the anomalous, strongly disordered regime there is qualitative disagreement. The SSG model[13] predicts no critical field. A model with a gasketlike backbone[12] predicts a field which decreases as the percolation threshold is approached, contrary to the experimental results. We show that this is expected to hold even for more realistic models with dead ends and a probability distribution for the loops. It is suggested that a backbone model which does not have a constant ramification number is probably required if the experiments are reliable.

We also briefly discuss the magnetic susceptibility. The difference between the low- and high-field regimes is pointed out. For the low-field situation the amplitude is constant and the behavior is that suggested by de Gennes.[3] At high fields the problem becomes nonlinear and sensitive to the geometry.

II. THE NETWORK EQUATIONS

On a thin strand the Landau-Ginzburg free-energy functional can be written[2]

$$F=A\,|\Delta|^2+\tfrac{1}{2}B\,|\Delta|^4+C\left|\hat{u}\left[i\vec{\nabla}-\frac{2e}{\hbar c}\vec{A}\right]\Delta\right|^2, \tag{2.1}$$

where $\hat{u}$ is a unit vector tangential to the strand. This leads to the Landau-Ginzburg (LG) equation

$$\left[-1/\xi_s^2+\left[i\frac{\partial}{\partial s}-\kappa\right]^2+b\,|\Delta|^2\right]\Delta=0\ , \tag{2.2}$$

where

$$s=(\hat{u}\cdot\vec{r})\ ,\quad \kappa=(2e/\hbar c)(\hat{u}\cdot\vec{A})\ , \tag{2.3}$$

and

$$1/\xi_s^2=-A/C\propto(T_c-T)/T_cD_0\ . \tag{2.4}$$

As usual,[15] we have assumed C proportional to the diffusion constant on the strand (D_0).

To describe a network we have to supplement the solutions of (2.2) on the branches by matching conditions at the junctions. First, continuity requires

$$\Delta_{ij}(i)=\Delta_i\ ,\quad \Delta_{ij}(j)=\Delta_j\ , \tag{2.5}$$

i.e., the order parameter on a branch must have the right values at the terminating junctions. In addition, one has a "Kirchoff" matching condition on the derivatives,[2]

$$\sum_j\left[\left[i\frac{\partial}{\partial s_{ij}}-\kappa_{ij}\right]\Delta_{ij}(s)\right]_i=0\ , \tag{2.6}$$

where all derivatives (and κ) are in the outgoing direction on the respective branches. The summation is over all branches irrespective of their other end. Thus distinct branches terminating in the same j are counted separately in Eq. (2.6). We note that Eq. (2.6) assumes all branches to have the same thickness and intrinsic correlation length (ξ_s).

In principle, one can now solve Eqs. (2.2) on each branch with the boundary conditions (2.5) and use the result to express the Kirchoff condition (2.6) in terms of the junction amplitudes (Δ_i,Δ_j). This is analogous to writing the electrical network equations in terms of the junction voltages (eliminating the currents).

For the problems in which we are interested the penetration depth is always large. We are therefore interested only in determining the (low-temperature) critical field H_{c2}. For homogeneous systems this is usually determined by the requirement that the amplitude $|\Delta|$ vanishes at the critical field. The LG Eq. (2.2) can then be linearized:

$$\left[-1/\xi_s^2+\left[i\frac{\partial}{\partial s}-\kappa\right]^2\right]\Delta=0\ , \tag{2.7}$$

and the solution with the boundary conditions (2.5) is

$$\Delta_{ij}(s)=\left[\Delta_i\frac{\sin(l_{ij}-s)/\xi_s}{\sin\theta_{ij}}+\Delta_j e^{i\gamma_{ij}}\frac{\sin(s/\xi_s)}{\sin\theta_{ij}}\right]e^{-i\kappa_{ij}s}\ , \tag{2.8}$$

where we use the notation of Ref. 2,

$$\theta_{ij}=l_{ij}/\xi_s\ , \tag{2.9}$$

$$\gamma_{ij}=\int_i^j\kappa_{ij}ds\approx\kappa_{ij}l_{ij}\ , \tag{2.10}$$

and l_{ij} is the length of the branch connecting i and j.

Substitution in Eq. (2.6) gives the set of coupled linear equations

$$-\Delta_i\sum_j(\cot\theta_{ij})/\xi_s+\sum_j(\Delta_j e^{i\gamma_{ij}}/\xi_s\sin\theta_{ij})=0\ . \tag{2.11}$$

Equations (2.11) are the basic network equations whose solution we shall consider in the rest of this paper. The formal structure of these equations is very similar to that arising in other physical problems on the same net. We shall discuss this in Sec. III.

The use of the linearized LG equations to determine a critical field assumes that there are superconducting states for all smaller fields. These are, however, states for which the amplitude $|\Delta|$ is finite and should be described by solutions of the nonlinear equations [Eq. (2.2)]. Equation (2.8) cannot be regarded as an adequate approximation for these solutions at small fields. We emphasize this point because we shall find that strongly disordered systems cannot be regarded as homogeneous in the usual way. As for arrays of Josephson junctions macroscopic coherence is destroyed by breaking the system into incoherent superconducting clusters. While we shall be able to demonstrate that this breaking up occurs it is important to realize that the formalism of Eqs. (2.11) is not adequate in describing these situations.

It will be convenient to generalize Eqs. (2.11) somewhat by considering the manifold of solutions of the inhomogeneous linear equations related to Eq. (2.7) on the branches. Formally, this amounts to replacing $1/\xi_s$ by q:

$$0<q<1/\xi_s \ , \quad q^2=1/\xi_s^2-\epsilon \tag{2.12}$$

in Eqs. (2.11) and (2.9). This retains the structure of the network equations and provides a manifold of solutions (parametrized by q) which go continuously to the solutions of (2.11). The solutions are related variationally to the true solutions one would obtain using Eq. (2.2). In several cases we shall use the inhomogeneous equations to demonstrate that a network has no critical field or to set a lower bound on the critical field.

It is useful to try to supplement the network equations (2.11) by suitable expressions for the free energy. In principle, the free energy is a property of the branches. An expression in terms of the junction amplitudes thus requires the substitution of the solutions of Eqs. (2.2), with proper boundary conditions (2.5) in the branch free-energy functional (2.1). In general, the expressions obtained in this way are complex and, in particular, are not simply related to the bilinear functional (in the Δ_i) from which Eqs. (2.11) can be obtained variationally. This is true even for homogeneous systems close to H_{c2} when the θ_{ij} are not small. One obtains useful expressions when one can expand the trigonometric functions, i.e., when

$$\theta_{ij},\gamma_{ij} \ll 1 \ , \tag{2.13}$$

and the geometry of the net is such that a gradient expansion of the Δ_i is justified. One then finds by expansion of (2.11) or directly from (2.1),

$$F=\alpha A\,|\,\Delta\,|^2+\beta C\,|\,[i\vec{\nabla}-(2e/\hbar c)\vec{A}]\Delta\,|^2 \ , \tag{2.14}$$

i.e., a renormalized free-energy functional where

$$\alpha \propto \tfrac{1}{2}\left\langle \sum_j l_{ij} \right\rangle , \tag{2.15}$$

$$\beta \propto \langle r_{ij}^2/l_{ij} \rangle \ , \tag{2.16}$$

and A and C are material constants on the branches [as in (2.1)]. It can be seen that α represents the effect of the finite-volume fraction of superconducting material and β the effect on the diffusion constant of the fact that one has to go a distance l_{ij} along the branches to connect points separated by r_{ij}. The procedure leading to (2.14) can be generalized to situations where Eqs. (2.11) have to be renormalized before proceeding to the continuum limit.

III. MAPPING ON SOME OTHER PROBLEMS

We first note that the amplitude fluctuations in the superconducting state (i.e., for large Δ) obey equations which are very similar to Eqs. (2.11) with the fluctuation energy

$$\epsilon \propto q^2 \tag{3.1}$$

replacing $1/\xi_s^2$. These correspond to a linearization of Eqs. (2.2) around the constant-amplitude equilibrium solution. A detailed derivation will be presented elsewhere.[16]

To bring out the relationship to other problems it is useful to rewrite Eqs. (2.11) in the form

$$m_i\Delta_i/\xi_s^2+\sum_j d_{ij}(\eta_{ij}\Delta_j-\Delta_i)=0 \ , \tag{3.2}$$

where we have defined a "bond diffusivity"

$$d_{ij}=(\xi_s \sin\theta_{ij})^{-1}\approx l_{ij}^{-1} \tag{3.3a}$$

and mass

$$m_i=\xi_s\sum_j \tan(\theta_{ij}/2)\approx \sum_j (l_{ij}/2) \ , \tag{3.3b}$$

and have defined

$$\eta_{ij}=e^{i\gamma_{ij}} \ . \tag{3.4}$$

The right-hand side (rhs) of Eqs. (3.3) follows for $\theta_{ij}\ll 1$. Thus the d_{ij} behave like bond conductances. Similarly m_i is proportional to the mass associated with the vertex i.

Consider first some cases for which $\eta_{ij}=1$. In the limit $\xi_s^2\to\infty$ the equations become identical to those of a resistor network when the Δ_i are replaced by site voltages (V_i). Thus in this limit the d_{ij} renormalize like a bond conductance and are simply related to the conductivity. We note that this limit constitutes a fixed point of the equations. If the m_i and γ_{ij} are initially zero they cannot be generated by the renormalization of the equations on any network.

The master equation for a diffusion problem again has the exact form of Eq. (3.2). An example would be de Gennes's ant in a labyrinth.[17] The Δ_i are chemical potentials or, equivalently, site-occupation probabilities. ξ_s^{-2} is, e.g., a Laplace-transform variable (ω) with the dimensions of frequency. m_i measures the volume associated with vertex i.

A completely equivalent problem is a resistor network with unit capacitors to ground from all lattice sites (see, e.g., Ref. 18). One also would obtain the same equations for the elastic properties of dry gels when the inertial terms are dominated by the network mass. (In practice, the solvent usually dominates and its mass does not scale.)

For all of these problems one is usually interested in the low-frequency limit, i.e., in the notation of Eq. (3.2) in situations where

$$m/(d\xi_s^2) \ll 1 \ . \tag{3.5}$$

This is the vicinity of the resistive fixed point ($m=0$) discussed above and in Secs. VI and VII.

A second class of problems which can be mapped exactly on these equations are solutions of the (single-particle) Schrödinger equations. Replacing

$$1/\xi_s^2 \to 2m\epsilon \tag{3.6}$$

in Eq. (2.7) gives the Schrödinger equation for free particles on the strands. The matching conditions at the junctions are also given by Eq. (2.6) (see, e.g., Ref. 19). The only difference would be in the treatment of the boundary conditions at the open ends. For electrons it is not always appropriate to use (2.11) there but this is a fairly minor point. The model is in essence a generalization of the random Kronig-Penney model in one-dimension (1D) studied extensively recently because of its relevance to localization in 1D.[20,21] We note that it is straightforward to add a junction scattering potential (see, e.g., Ref. 19).

Very similar equations arise in the electronic tight-binding model. We note that this approach emphasizes the geometrical randomness rather than the potential and thus provides a different approach to the properties of random systems which may have advantages. We shall discuss this elsewhere.[22]

IV. FINITE NETS

A. A superconducting ring

As an illustration it is useful to start by discussing the trivial problem of a superconducting ring (of circumference L).[11] One can formally introduce a vertex on the ring and Eqs. (2.11) become

$$(-2\cot\theta_L + 2\cos\gamma/\sin\theta_L)\Delta = 0 \tag{4.1}$$

or

$$\cos\theta_L = \cos\gamma \ . \tag{4.2}$$

It is important to recall that the linearized Landau-Ginzburg equation [Eq. (2.7)] implicitly assumes that the system is driven normal by the field. Thus the value

$$\theta_L = L/\xi_s \tag{4.3}$$

is actually the maximum value consistent with the existence of superconductivity. Thus Eq. (4.2) predicts a critical field only when

$$L/\xi_s = \theta_L < 2\pi \ . \tag{4.4}$$

For larger rings the left-hand side (lhs) of Eq. (4.2) can take all values between -1 and $+1$ and the ring cannot be driven normal by a magnetic field. This is of course the usual situation envisaged in flux quantization experiments. We note that the amplitude $|\Delta|$ is constant in this case so that the exact solution of Eq. (2.2) is essentially trivial for all values of θ and γ.[11]

B. A ring with a side branch

When applied to the case considered there one recovers the results of Ref. 2. Consider a circular loop of circumference L with an open side branch of length L_{12} joined to it. There are two junctions—the point where the branch is connected (Δ_1) and the end of the open branch (Δ_2).

Thus from Eq. (2.9),

$$-\Delta_2\cot\theta_{12} + \Delta_1/\sin\theta_{12} = 0 \ , \tag{4.5a}$$

$$-\Delta_1(2\cot\theta_L + \cot\theta_{12}) + 2\Delta_1\cos\gamma/\sin\theta_L + \Delta_2/\sin\theta_{12} = 0 \ , \tag{4.5b}$$

where

$$\theta_L = L/\xi_s \ , \quad \theta_{12} = L_{12}/\xi_s \ , \tag{4.6}$$

and γ is proportional to the flux through the loop.

This leads to Eq. (12) of Ref. 2,

$$\cos\theta_L - \tfrac{1}{2}\sin\theta_L\tan\theta_{12} = \cos\gamma \ . \tag{4.7}$$

For large ξ_s this becomes

$$\theta_L(\theta_L + \theta_{12}) = L(L + L_{12})/\xi_s^2 = \gamma^2 \ . \tag{4.8}$$

Thus the critical field is increased. When the θ become large there is no critical field. The smallest value of ξ_s for which there is a critical field is given by

$$\cos\theta_L - \tfrac{1}{2}\sin\theta_L \tan\theta_{12} = -1 \ . \tag{4.9}$$

One notices that this is dominated by the side branch (θ_{12}) when it is long.

C. A line with side branches

A more general case is that of many open, dead-end, side branches. This is obviously relevant to solutions on percolation clusters. We consider a "transmission line" problem (Fig. 1)—i.e., a string connecting junctions O and N with open side branches (of length l_i) connected at the intermediate junctions ($i = 1, \ldots, N-1$). Thus at the junction i,

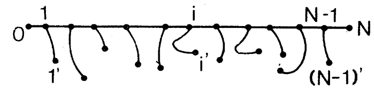

FIG. 1. Line with dead-end side branches.

$$-(\cot\theta_{i,i+1} + \cot\theta_{i-1,i})\Delta_i + \eta_{i,i-1}\Delta_{i-1}/\sin\theta_{i,i-1} + \eta_{i,i+1}\Delta_{i+1}/\sin\theta_{i,i+1} = \cot\theta_i \Delta_i - \Delta_{i'}(e^{i\gamma_i}/\sin\theta_i) \ , \tag{4.10a}$$

$$\Delta_{i'}\cot\theta_i = \Delta_i(e^{-i\gamma_i}/\sin\theta_i) \ , \tag{4.10b}$$

where

$$\theta_{i,i+1} = L_{i,i+1}/\xi_s \ , \quad \theta_i = l_i/\xi_s \ ,$$

and the $\eta_{ij'}$ are defined analogously. Eliminating the open-end amplitudes and using elementary trigonometric identities this can be written

$$m_i\Delta_i + d_{i,i-1}(\eta_{i,i-1}\Delta_{i-1} - \Delta_i) + d_{i,i+1}(\eta_{i,i+1}\Delta_{i+1} - \Delta_i) = 0 \ , \tag{4.11}$$

where we have defined (as in Sec. III)

$$m_i = \tan(\theta_{i,i+1}/2) + \tan(\theta_{i,i-1}/2) + \tan\theta_i \ , \tag{4.12a}$$

$$d_{ij} = (\sin\theta_{ij})^{-1} \ , \tag{4.12b}$$

$$\eta_{ij} = \eta_{ji}^{\dagger} = \exp i\gamma_{ij} \ . \tag{4.13}$$

The ends of the string will have a term

$$F_0 = (\cot\theta_{01})\Delta_0 + \Delta_1\eta_{01}/\sin\theta_{01} \tag{4.14}$$
$$= -m_{01}\Delta_0 + d_{01}(\eta_{01}\Delta_1 - \Delta_0) \ ,$$

where F_0 represents terms in Eqs. (2.11) resulting from any other branches attached at 0. We want to eliminate the Δ_i from Eqs. (4.11) to obtain an effective coupling representing the properties of the line. We notice that, because of the term $\tan\theta_i$ in Eq. (4.12a), Eqs. (4.11) are different from the original form of Eqs. (2.11). The trigonometric relationships between the coefficients do not hold and this cannot be remedied by redefining θ_{ij}. We start at one end and successively eliminate the Δ_i. One finds

$$d_{n0} = d_{0n} = \frac{d_{0,n-1}d_{n-1,n}}{d_{0,n-1} + d_{n-1,n} - \bar{m}_{n-1}} \ , \tag{4.15a}$$

$$\bar{m}_n = m_n + \frac{\bar{m}_{n-1}d_{n-1,n}}{d_{0,n-1} + d_{n-1,n} - \bar{m}_{n-1}} \ , \tag{4.15b}$$

and

$$(\bar{m}_0)_n = (\bar{m}_0)_{n-1} + \bar{m}_n - m_n \ . \tag{4.15c}$$

The phase factors are additive

$$\eta_{0n} = \prod_1^n \eta_{i-1,i} \ , \tag{4.16}$$

These expressions are presented to demonstrate the role of the dead-end side branches. If one had no side branches one would obviously find

$$d_{n0} = (\sin\theta_{0n})^{-1} \ , \tag{4.17}$$

and the effect of (4.15b) and (4.15c) would be to replace $\tan(\frac{1}{2}\theta_{0,(n-1)})$ by $(\frac{1}{2}\theta_{0,(n-1)})$ by $\tan(\theta_{0n}/2)$ in the expression for the m_i [Eq. (4.12a)]. The implied phase coherence disappears when there are side branches.

Consider the case where ξ_s is large, so that the θ_{ij} are small initially. One can then expand in Eqs. (4.12) and interpret ξ_{sn} defined by the ratio

$$\bar{m}_n/d_{n0} = (L_n/\xi_{sn})^2 \tag{4.18}$$

as an effective coherence length for the line on scale L_n. This is, of course, also the natural expansion parameter in Eqs. (4.15). One notes that the dead ends affect the $\bar{m}$ to zero order [Eqs. (4.15b) and (4.15c)] and the d only to first order.

There are therefore two effects of the dead ends:

(1) The coherence length is reduced, essentially in the same way one would find if one included the full mass density in the Landau-Ginzburg free-energy functional.

(2) The phase coherence is destroyed.

We demonstrate the importance of these effects in the example in the next section.

D. A ring with many side branches

Consider a ring of circumference L with N equally spaced side branches all of equal length l (see Fig. 2). The problem is periodic and the solution of Eqs. (4.11) is immediate.

One finds

$$\cos[(2\pi m+\gamma)/N] = \cos(L/N\xi_s) - \tfrac{1}{2}\sin(L/N\xi_s)\tan(l/\xi_s) , \quad (4.19)$$

where

$$\gamma = 2\pi\Phi/\Phi_0 , \quad (4.20)$$

where Φ is the flux through the ring and the relevant solution is

$$\Delta_j = \Delta \exp[2\pi i (mj/N)] . \quad (4.21)$$

For $N=1$ one regains Eq. (4.7). We are, however, interested in large N. For large N one can expand (4.19) giving

$$(2\pi m+\gamma)^2 = L(L+Nl)/\xi_s^2 , \quad (4.22)$$

which is valid as long as

$$(2\pi m+\gamma)/N ,\ \ L/N\xi_s ,\ \ l/\xi_s \ll 1 . \quad (4.23)$$

This is in agreement with the renormalization of the coherence length [Eq. (4.18)].

We note that m describes the winding number of the phase around the ring and is thus related to flux quantization. An analogous index shows up for the uniform ring (Sec. IV A). One would, however, expect that the discreteness of the solutions imposed by the side branches would modify the hysteretic effects. This would be even more pronounced when the side branches are not uniform so that considerable configurational barriers appear in transitions between different branches of solutions.

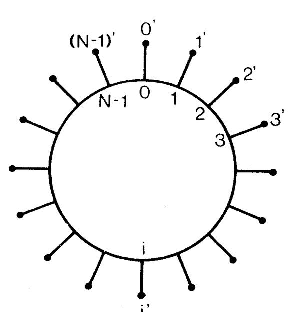

FIG. 2. Ring with equally spaced dead-end side branches of equal length.

E. A Double loop

A different class of problems arises when one has interconnected loops. We consider the two-loop configuration of Fig. 3. There are two vertices (1,2) connected by three branches (I,II,III) of lengths $L_{\rm I}$, $L_{\rm II}$, and $L_{\rm III}$, respectively.

One has two equations,

$$-\Delta_1(\cot\theta_{\rm I}+\cot\theta_{\rm II}+\cot\theta_{\rm III}) + \Delta_2(\eta_{\rm I}/\sin\theta_{\rm I}+\eta_{\rm II}/\sin\theta_{\rm II} + \eta_{\rm III}/\sin\theta_{\rm III}) = 0 , \quad (4.24a)$$

$$\Delta_1(\eta_{\rm I}^\dagger/\sin\theta_{\rm I}+\eta_{\rm II}^\dagger/\sin\theta_{\rm II}+\eta_{\rm III}^\dagger/\sin\theta_{\rm III}) - \Delta_2(\cot\theta_{\rm I}+\cot\theta_{\rm II}+\cot\theta_{\rm III}) = 0 , \quad (4.24b)$$

where

$$\theta_{\rm I} = L_{\rm I}/\xi_s,\ \ \theta_{\rm II} = L_{\rm II}/\xi_s,\ \ \theta_{\rm III} = L_{\rm III}/\xi_s , \quad (4.25)$$

and

$$\eta_{\rm I} = e^{i\gamma_{\rm I}},\ \ \eta_{\rm II} = e^{i\gamma_{\rm II}},\ \ \eta_{\rm III} = e^{i\gamma_{\rm III}} . \quad (4.26)$$

The general case gets quite complicated. Assume first a symmetrical situation

$$\theta = \theta_{\rm I} = \theta_{\rm III},\ \ \gamma_{\rm I} - \gamma_{\rm II} = \gamma_{\rm II} - \gamma_{\rm III} = \gamma . \quad (4.27)$$

The condition for the existence of solutions is

$$2\cot\theta + \cot\theta_{\rm II} = \pm[2(\cos\gamma/\sin\theta) + 1/\sin\theta_{\rm II}] . \quad (4.28)$$

We only discuss the role of the internal branch. For strong coupling,

$$\theta_{\rm II} \ll \theta,\ \ \theta_{\rm II} \ll 1 , \quad (4.29)$$

one has to choose the plus sign in (4.28),

$$\cos\theta - \tfrac{1}{2}\sin\theta\,\tan(\theta_{\rm II}/2) = \cos\gamma , \quad (4.30)$$

similar to Eq. (4.7). Since γ is the flux through a half loop the two halves are in essence independent. For weak coupling,

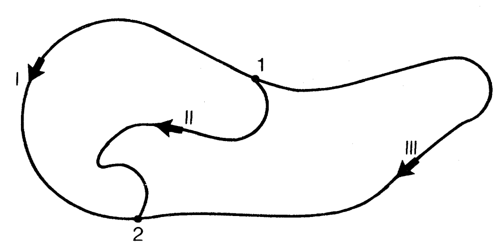

FIG. 3. Two coupled loops.

$$|\pi-\theta_{\rm II}| \ll 1 , \qquad (4.31)$$

one has to choose the second solution,

$$\cos\theta+\tfrac{1}{2}\sin\theta\cot\theta_{\rm II}/2=-\cos\gamma , \qquad (4.32)$$

as for a loop with no internal branch.

A second case we want to consider is

$$\theta_{\rm I}=\theta_{\rm II}=\theta_{\rm III}=\theta ,$$
$$\gamma_{\rm I}-\gamma_{\rm II}=\gamma, \ \ \gamma_{\rm II}-\gamma_{\rm III}=2\gamma . \qquad (4.33)$$

The total flux is 3γ. Thus

$$9\cos^2\theta=3+2(\cos\gamma+\cos2\gamma+\cos3\gamma) , \qquad (4.34)$$

which can be written

$$\tfrac{1}{4}(9\cos^2\theta-1)=2\cos^3\gamma+\cos^2\gamma-\cos\gamma . \qquad (4.35)$$

This exhibits an interesting new behavior. The lhs is monotonic (in $\cos^2\theta$) but the rhs has a minimum and a maximum. In the range

$$0.94<\theta<1.23, \ \ \tfrac{1}{9}\le\cos^2\theta<0.346 \qquad (4.36)$$

there are three critical fields. Superconductivity disappears at H_1 (on the lowest branch), reappears at H_2, and disappears again at H_3 (for each half-period of $\cos\gamma$). In the range

$$1.23<\theta<1.37, \ \ 0.04<\cos^2\theta<\tfrac{1}{9} \qquad (4.37)$$

there are two critical fields. Finally, for

$$1.37<\theta, \ \ \cos^2\theta<0.04 \qquad (4.38)$$

there is no critical field.

V. THE SQUARE LATTICE

We consider a square lattice consisting of superconducting strands of constant length (a) joined at the lattice points. For convenience we choose a Landau gauge

$$A_x=A_z=0, \ \ A_y=Hx . \qquad (5.1)$$

We can multiply the equation by the constant factor $\sin\theta$. Thus at the junction nm of the lattice Eq. (2.11) becomes

$$0=-4\Delta_{n,m}\cos\theta+\Delta_{n+1,m}+\Delta_{n-1,m}$$
$$+e^{i\gamma n}\Delta_{n,m+1}+e^{-i\gamma n}\Delta_{n,m-1} , \qquad (5.2)$$

where

$$\theta=a/\xi_s \qquad (5.3)$$

and

$$\gamma=2\pi Ha^2/\Phi_0 . \qquad (5.4)$$

As in the analogous electron problem, we write

$$\Delta_{nm}=f_q(n)e^{iqm} . \qquad (5.5)$$

Substitution in Eq. (5.2) gives

$$[-4\cos\theta+2\cos(\gamma n+q)]f_q(n)$$
$$+f_q(n+1)+f_q(n-1)=0 . \qquad (5.6)$$

Thus the problem reduces to the "incommensurate" 1D tight-binding problem

$$2\cos(\gamma n+q)f_n+f_{n+1}+f_{n-1}=\epsilon f_n , \qquad (5.7)$$

which has been studied by several authors,[5–9] most recently by Aubry.[10] We note the close relationship to the behavior of band electrons in a magnetic field pointed out by Azbel[6] (see also Refs. 7–9). In Eq. (5.6) we are, however, only interested in the special solution

$$\epsilon=4\cos\theta . \qquad (5.8)$$

The critical field (H_{c2}) is reached when γ is such that this special solution is equal to ϵ at the band edge of the spectrum of Eq. (5.7).

The spectrum has been studied in great detail by Hofstadter.[9] We only note three properties:

(a) There are no eigenvalues outside the range

$$-4\le\epsilon\le4 . \qquad (5.9)$$

(b) The spectrum is symmetric in γ (and ϵ).

(c) There is invariance under the transformation

$$\gamma\to\gamma+2\pi . \qquad (5.10)$$

Adding a flux quantum per square has no effect.

Because of the above, it is sufficient to consider

$$\gamma\le\pi . \qquad (5.11)$$

For small γ we can estimate the position of the band edge by expanding around the maxima of the periodic potential $[2\cos(\gamma n+q)]$ in Eq. (5.7). This gives

$$\gamma^2n^2f_n-2f_n+f_{n+1}+f_{n-1}=4(\cos\theta-1)f_n . \qquad (5.12)$$

Or in a continuum approximation

$$[-\gamma^2(x/a)^2+a^2\partial^2/\partial x^2]f(x)=4(\cos\theta-1)f(x) , \qquad (5.13)$$

where $x=na$.

The highest eigenvalue of the harmonic-oscillator equation on the rhs of (5.13) is at $-\gamma$ leading to

$$\gamma=4(1-\cos\theta) . \quad (5.14)$$

Overlap terms between the harmonic-oscillator functions on adjacent extrema are small, so one expects the approximation to be fairly reliable over most of the range (see, however, below).

Equation (5.14) can be written

$$H_{c2}(a)=(4\Phi_0/\pi a^2)\sin^2(a/2\xi_s) , \quad (5.15)$$

where we have substituted the definitions of θ [Eq. (5.3)] and γ [Eq. (5.4)] in Eq. (5.14). Expanding the rhs ($a/2\xi_s \ll 1$) gives

$$H_{c2}\approx(\Phi_0/\pi\xi_s^2)\{1-O[(a/\xi_s)^2]\} , \quad (5.16)$$

i.e., the continuum result.

The behavior predicted for large values of a/ξ_s is, at first sight, surprising. The harmonic-oscillator solutions we have considered lose their meaning when a/ξ_s becomes too large. This results from the fact that the bandwidth of Eq. (5.7) is periodic in γ with period 2π [see (c) above]. There is therefore a minimum bandwidth—say, $2\epsilon_c$. It follows that Eq. (5.6) has solutions for all values of γ when

$$|4\cos\theta| < \epsilon_c . \quad (5.17)$$

There is no critical field. The origin of this is the periodicity in γ which reflects flux quantization. Adding one flux quantum per square leaves the equations invariant.

At the critical value one has

$$\gamma=\gamma_c,\ \ H_{c2}^c=\gamma_c\Phi_0/2\pi a^2 , \quad (5.18)$$
$$\cos^2(a/\xi_s)=(\epsilon_c/4)^2 ,$$

where γ_c is the value of γ for which the bandwidth is minimal (ϵ_0). From the results of Ref. 9 (Fig. 1) and (5.18) one finds

$$\gamma_c\approx 0.83\pi \quad (5.19)$$

and

$$\epsilon_c^2\approx 6.7,\ \ \theta_c=(a/\xi_s)_c\approx 0.87 . \quad (5.20)$$

Finally, combining Eqs. (5.18)—(5.20),

$$(H_{c2})_c\approx 1.72\Phi_0/\pi\xi_s^2\approx 0.4\Phi_0/a^2 , \quad (5.21)$$

which is somewhat larger than the bulk critical field. Since Eq. (5.15) predicts a critical field which is always smaller than the bulk field it is obvious that the approximation is no longer accurate. This can also be seen from the structure in the position of the band edge in Fig. 1 of Ref. 9.

Physically, the predicted behavior is thus similar to that of a ring (Sec. IV A). When θ_c exceeds the value indicated in Eq. (5.20) one should observe Little-Parks[11] oscillations but the net cannot be driven normal by a magnetic field. As we have noted repeatedly the superconducting solutions are then not described adequately by the linear approximation. The calculation of H_{c2}^c and θ_c is, however, correct.

The generalization of the above to a three-dimensional lattice is straightforward and essentially trivial. As in the continuous case variation of the order parameter parallel to the field can only increase the free energy and is therefore unfavorable.

VI. THE TRIANGULAR SIERPINSKI GASKET

Gefen *et al.*[12] have recently suggested a model for the backbone of percolation clusters which seems to give reasonable results for the diffusion constant and for the density of the backbone. The idea is to study the properties of self-similar structures with anomalous dimensions as a model for the backbone of the infinite cluster at p_c. The properties of finite clusters or of the infinite cluster for $p>p_c$ are then determined by introducing suitable crossovers. The model has the additional attraction that it contains a hierarchy of loops and should therefore avoid the anomalies associated with the unique loop size which we encountered in Sec. V. We shall therefore solve the linearized Landau-Ginzburg equation on a plane triangular Sierpinski gasket. The gasket is described in Fig. 4.

A. Iteration procedure

The basic unit of the construction is an equilateral triangle with bonds connecting the centers of the edges. Three such triangles are then used to construct a new triangle of twice the size with a hole in the middle. The procedure can be continued (see Fig. 4). We want to solve Eqs. (2.11) on such a network. The basic procedure is to eliminate at each stage the junctions at the centers of the edges and obtain a new set of effective equations in terms of the Δ at the vertexes of the triangle. These can then

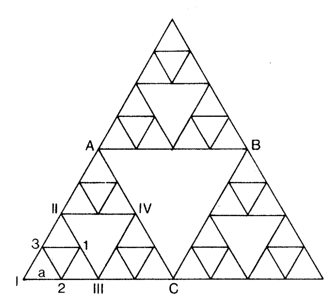

FIG. 4. Triangular Sierpinski gasket. The labeling of the vertices is that used in Secs. VI and VIII.

be used in the next stage of the iteration. The procedure can be carried out exactly. The three equations at the vertices of an equilateral triangle (e.g., 123 in Fig. 4) can be written in matrix form

$$p\hat{T}_{123}\underline{\Delta}=\underline{F} , \tag{6.1}$$

where $\hat{T}$ takes care of all terms in the relevant equations resulting from internal branches and $\underline{F}$ describes all the other terms (e.g., those related to coupling between vertex $\underline{1}$ and the external vertices II and III). If we know $\hat{T}$ for the smallest triangles we can use it to eliminate the internal vertices and calculate an effective $\hat{T}$ involving only the external vertices of these triangles.

Consider first a single triangle (apexes 1,2,3). Equations (2.11) and (6.1) define a matrix

$$\hat{T}_{123}=\begin{bmatrix} -2t & \eta_{12} & \eta_{13} \\ \eta_{21} & -2t & \eta_{23} \\ \eta_{31} & \eta_{32} & -2t \end{bmatrix} , \tag{6.2}$$

where

$$t_0=\cos\theta,\quad \eta_{ij}^{0}=\eta_{ji}^{0\dagger}=e^{i\gamma_{ij}} \tag{6.3}$$

are initially defined as in Eqs. (2.9) and (2.10). Also

$$p_0=(\sin\theta)^{-1} . \tag{6.4}$$

Note that the factors $(\sin\theta)^{-1}$ in Eqs. (2.11) can be factored out. In the limit $t=\eta=1$ they scale like the bond resistances.

To iterate we consider a triangle with bonds connecting the edge centers. We define two vectors,

$$\underline{\Delta}^{a}=\begin{bmatrix} \Delta_{\rm I} \\ \Delta_{\rm II} \\ \Delta_{\rm III} \end{bmatrix},\quad \underline{\Delta}^{c}=\begin{bmatrix} \Delta_1 \\ \Delta_2 \\ \Delta_3 \end{bmatrix} , \tag{6.5}$$

where Roman numerals label the apexes $(\vec{\Delta}^{a})$ and $(\vec{\Delta}^{c})$ describes the edge centers so that Δ_1 is the center of II-III, etc. (Fig. 4). The equations for the a vertices can now be written

$$\underline{F}=\hat{U}_n\underline{\Delta}^{c}-2t_n\underline{\Delta}^{a} , \tag{6.6a}$$

where, as in Eqs. (6.1), $\underline{F}$ describes all terms in Eqs. (2.11) due to bonds not belonging to the triangle considered. For the other three (c) vertices, one has

$$\hat{A}_n\Delta^{c}=\hat{U}_n^{\dagger}\underline{\Delta}^{a} , \tag{6.6b}$$

and we have defined

$$\hat{A}_n=-\hat{T}_{123}^{n}+2t_n\hat{I} \tag{6.7}$$

($\hat{I}$ the unit matrix) and

$$\hat{U}_n=\begin{bmatrix} 0 & \eta_{\rm I2}^{n} & \eta_{\rm I3}^{n} \\ \eta_{\rm II1}^{n} & 0 & \eta_{\rm II3}^{n} \\ \eta_{\rm III1}^{n} & \eta_{\rm III2}^{n} & 0 \end{bmatrix} . \tag{6.8}$$

Solving (6.6b) for Δ^{c} and substituting in (6.6a) gives the iterative expression

$$\hat{T}_{n+1}=C_n(\hat{U}_n\hat{A}_n^{-1}\hat{U}_n^{\dagger}-2t_n\hat{I}) , \tag{6.9a}$$

$$p_{n+1}=P_n/C_n . \tag{6.9b}$$

The proportionality factor (C_n) should be such that

$$\eta_{ij}^{n+1}=\exp i\gamma_{ij}^{n+1} \quad (\gamma \text{ real}) . \tag{6.10}$$

The calculation is immediate but somewhat cumbersome. It is convenient to define renormalized fluxes

$$\bar{\eta}_n=\exp i\bar{\gamma}_n=\eta_{12}^{n}\eta_{23}^{n}\eta_{31}^{n} \tag{6.11a}$$

and

$$\begin{aligned}\eta_n=\exp i\gamma_n&=\eta_{13}^{n}\eta_{32}^{n}\eta_{21}^{n}\\ &=\eta_{\rm III1}^{n}\eta_{13}^{n}\eta_{3\rm II}^{n}=\eta_{\rm II2}^{n}\eta_{21}^{n}\eta_{1\rm II}^{n} .\end{aligned} \tag{6.11b}$$

Initially one has

$$\gamma_0=\bar{\gamma}_0=2\pi\Phi^{0}/\Phi_0=\frac{\pi\sqrt{3}a^{2}H}{2\Phi_0} , \tag{6.12}$$

where Φ^{0} is the flux through the smallest triangles (of edge a). We assume a uniform field and γ_0 is obviously gauge invariant. We also define

$$a_n=16t_n^{2}-1+4t_n\cos\gamma_n+\cos(\gamma_n+\bar{\gamma}_n) , \tag{6.13}$$

$$\begin{aligned}b_n&=|b_n|e^{-i\varphi_n}\\ &=16t_n^{2}-1+4t_n(2e^{-i\gamma_n}+e^{-i(2\gamma_n+\bar{\gamma}_n)})\\ &\quad+e^{-2i\gamma_n}+2e^{-i(\gamma_n+\gamma_n)} ,\end{aligned} \tag{6.14}$$

and the determinant of A_n [Eq. (6.7)],

$$\det\hat{A}_n=64t_n^{3}-12t_n-2\cos\bar{\gamma}_n . \tag{6.15}$$

One finds

$$t_{n+1}=(t_n\det\hat{A}_n-a_n)/|b_n| , \tag{6.16}$$

$$p_{n+1}=(|b_n|/\det\hat{A}_n)p_n , \tag{6.17}$$

and for the phase factors,

$$\eta_{ij}^{n+1}=\exp i\gamma_{ij}^{n+1} , \tag{6.18}$$

where

$$\gamma_{\mathrm{I\,II}}^{n+1}=\gamma_{\mathrm{I3}}^{n}+\gamma_{\mathrm{3II}}^{n}-\varphi_n \, ,$$
$$\gamma_{\mathrm{II\,III}}^{n+1}=\gamma_{\mathrm{III}}^{n}+\gamma_{\mathrm{1III}}^{n}-\varphi_n \, , \tag{6.19}$$
$$\gamma_{\mathrm{III\,I}}^{n+1}=\gamma_{\mathrm{III2}}^{n}+\gamma_{\mathrm{2I}}^{n}-\varphi_n \, ,$$

so that

$$\gamma_{n+1}=3\gamma_n+\overline{\gamma}_n-3\varphi_n \, , \tag{6.20}$$

$$\overline{\gamma}_{n+1}=4^{n+1}\gamma_0+3\sum_{i=1}^{n}2^{n-i}\varphi_n$$
$$=\tfrac{1}{2}(4^{n+1}\gamma_0+4\overline{\gamma}_n)+3\varphi_n \, . \tag{6.21}$$

Thus the effective flux through the corner triangles is reduced [(6.20)] but the flux through the central triangle is increased [(6.21)]. The net effect is that the effective flux through the renormalized triangle is smaller than its geometrical value, but is still proportional to the area because of the flux trapped in the central triangle ($\overline{\gamma}$).

B. Fixed-point expansions

It is useful to start by considering the situation in the absence of magnetic fields. Equation (6.16) becomes

$$t_{n+1}=t_n(4t_n-3) \, , \tag{6.22}$$

and from (6.17),

$$p_{n+1}/p_n=(2t_n+1)/(4t_n+1)(2t_n-1) \, . \tag{6.23}$$

There are two fixed points to Eq. (6.22) at $t=0$ and at $t=1$. Both are unstable. One has a power-law behavior close to the fixed points, but for sufficiently large n, t always becomes large and increases exponentially with the dimensions

$$t_{n+1}\approx 4t_n^2, \;\; p_{n+1}\approx p_n/4t_n \, , \tag{6.24}$$

so that

$$\log t_n \approx -\log p_n \approx 2^n \, . \tag{6.25}$$

We mentioned in Sec. III that the $t=1$ fixed point is relevant to the resistor network and to low-frequency diffusion. It is also the only fixed point we shall discuss here. It describes situations where θ_0 is small. In principle, one could of course also have situations for which the $t=0$ fixed point plays a role initially (e.g., $\theta_0 \simeq \pi/2$). For special values of t_0 one can also cross over from one fixed point to the other. The crossover regime is, however, complicated and extremely erratic. For most initial values (t_0,γ_0) the crossover from the vicinity of the $t=1$ fixed point to the large-t regime [Eqs. (6.24) and (6.25)] is rapid and not interesting. We therefore disregard the $t=0$ fixed point and the crossover regime in the following discussion. We note, however, that this fixed point is of interest near the band edges in the electronic problems discussed in Sec. III. The fixed points of (6.22) are, we believe, the only fixed points of the renormalization process defined by Eqs. (6.16)–(6.21).

Consider now the behavior near the $t=1$ fixed point. If θ and γ are initially small (on the scale a) one can expand

$$t_n=\cos\theta_n \approx 1-\theta_n^2/2 \, , \tag{6.26a}$$

$$\eta_n \approx 1+i\gamma_n-\gamma_n^2/2 \, , \tag{6.26b}$$

with an analogous expansion for $\overline{\eta}_n$. Substituting in Eq. (6.14) gives

$$\varphi_n=\tfrac{2}{3}\gamma_n+\tfrac{1}{5}\overline{\gamma}_n \, , \tag{6.27}$$

and from (6.20),

$$\gamma_{n+1}=\gamma_n+\tfrac{2}{5}\overline{\gamma}_n \, , \tag{6.28a}$$

and from (6.21),

$$\overline{\gamma}_{n+1}=\frac{4^{n+1}}{2}\gamma_0+\tfrac{13}{5}\overline{\gamma}_n+2\gamma_n \, . \tag{6.28b}$$

In essence, this shows that corrections to γ_n are not important. It is straightforward to solve Eq. (6.27) and obtain explicit expressions for γ_n and $\overline{\gamma}_n$ in terms of γ_0. It is, however, found that

$$\gamma_n \approx \overline{\gamma}_n \approx 4^n\gamma_0 \, . \tag{6.29}$$

The detailed numerical factors are not interesting. We therefore use the approximation (6.29) below.

Expanding Eq. (6.16) one finds

$$\theta_{n+1}^2=5\theta_n^2-\tfrac{371}{450}\gamma_n^2 \tag{6.30}$$

as long as θ_n^2 and γ_n^2 are both small, i.e., in the vicinity of the $t=1$ ($\theta^2=\gamma^2=0$) fixed point. The effect of γ_n^2 in Eq. (6.30) is to increase the instability of the fixed point.

C. A finite gasket

Consider now a finite gasket of size

$$L=2^n a \, . \tag{6.31}$$

The gasket is renormalized to a ring (or single triangle) and one has the condition

$$\det\hat{T}_n=-8t_n^3+6t_n+2\cos\overline{\gamma}_n=0 \tag{6.32}$$

for the existence of solutions. There are no solutions (for any $\overline{\gamma}_n$) outside the range

$$-1\le t_n \le 1 \, . \tag{6.33}$$

Assume first that this inequality holds. We can then write

$$t_n = \cos\theta_n \ , \qquad (6.34)$$

and (6.32) becomes

$$\cos 3\theta_n = \cos\gamma_n \ . \qquad (6.35)$$

Moreover, we have to be close to the fixed point, i.e.,

$$0 \le \theta_n^2 \approx 5^n \theta_0^2 \lesssim 1 \ . \qquad (6.36)$$

Expanding (6.35) one finds

$$9\theta_n^2 \approx \gamma_n^2 \ , \qquad (6.37)$$

$$H_c \approx \Phi_0 / L\bar{\xi}_s \propto \Phi_0/(\xi_s L^{(1-\theta)/2}) \ , \qquad (6.38)$$

where we have defined a renormalized coherence length

$$\bar{\xi}_s^2 \propto (\tfrac{4}{5})^n \xi_s^2 \approx L^{-\theta} \xi_s^2 \ , \qquad (6.39)$$

where

$$\theta = (\ln 5)/(\ln 2) - 2 \approx 0.32 \ . \qquad (6.40)$$

The implied requirement that $\bar{\xi}_s$ should be, at least, comparable to $L(\sim 2^n)$ is obviously very restrictive. It is convenient to define a length from (6.36). We have

$$\lambda_s = \lambda(\xi_s/a) \propto (\xi_s/a)^{2/(2+\theta)} \ . \qquad (6.41)$$

λ_s is analogous to a diffusion length for "time" ξ_s^2. It is the range of correlations in Δ on the infinite gasket for solutions of the linear equations. As noted in Sec. III, λ_s is also, except for numerical factors, the coherence length for fluctuations in the superconducting state on the infinite gasket. We have shown that there are no solutions to the linearized equations for large gaskets when

$$\lambda_s < L \ . \qquad (6.42)$$

There are, obviously, low-field solutions on any gasket (in mean field). Thus superconducting coherence disappears at some critical field for which the local amplitudes $|\Delta|$ are still finite. Superconductivity disappears because long-range order (on the scale L) is destroyed, and not because $|\Delta|$ goes to zero locally. We have thus found that, because of the anomalous fractal structure of the gaskets they have a peculiar anomalous regime when ξ_s becomes *small*, so that (6.42) holds.

We can set a lower bound on the critical field in this regime by considering solutions of the inhomogeneous LG equations on the gasket. The size L defines a maximum value of $\theta(\theta_L)$:

$$\theta_L = q_L a \approx L^{-(2+\theta)/2} \ . \qquad (6.43)$$

This is the maximum curvature consistent with order on the scale L. In a thermodynamic theory it would enter into the finite-size effects. If one simply replaces θ_0 by θ_L in Eq. (6.46) one obtains identically,

$$\theta_n^2(\theta_L) \equiv 1 \ , \qquad (6.44)$$

and from (6.38),

$$H_L = H_c(L) \propto \Phi_0/L^2, \ \ \xi_s^{-1} > q_L \ , \qquad (6.45)$$

independent of ξ_s. This would be the critical field closer to T_c when $\xi_s = q_L^{-1}$. It is obviously a lower bound on the critical field.

We can also set an upper bound from the critical field of clusters of size $\lambda(\xi_s)$ [Eq. (6.41)],

$$H_s = H(\lambda_s) \propto \Phi_0/\lambda_s^2 \ . \qquad (6.46)$$

Any cluster larger than λ_s consists of smaller subunits of this size. Thus H_s is a field at which any cluster larger than (λ_s) becomes completely normal, and

$$H_L < H_c(L) < H_s \ . \qquad (6.47)$$

Qualitatively, one can also see how the critical field is determined. The transition to the normal state results from the competition between the kinetic energy of the supercurrents induced by the field and the free energy of the superconducting state. Up to a distance λ_s the amplitudes are strongly coupled. For larger clusters the fact that the current distribution is necessarily nonuniform becomes important. Thus all the currents associated with the closed loop ABC in Fig. 4 have to pass through these points (A,B,C). A region of size λ near point A therefore experiences a higher current density than a similar region near the vertex I and will be driven normal at a lower field. Such points whose origins are essentially geometric therefore act as weak links.

One therefore expects a large gasket to breakup into successively smaller units as the field is increased, until it is finally driven normal at a field H_s when the largest connected gaskets are of size $\lambda(\xi_s)$. For the infinite gasket this implies that an imposed field (H) determines a maximum loop size (ξ_H). Up to the scale ξ_H one retains the gasket structure. On a larger scale one has either separate clusters or a treelike connection with no loops. At the upper limit H_s the magnetic length ξ_H becomes equal to λ_s and gaskets of this size are driven normal uniformly. It is therefore natural to postulate a scaling behavior

$$\xi_H/\lambda_s = f(H/H_s) \propto (H/H_s)^{1/(2-y)} \ . \qquad (6.48)$$

We note that ξ_H is the maximum loop size consistent with field H and that it decreases as H is increased. A different way of writing (6.48) is

$$H \propto (\Phi_0/\xi_H^2)(\xi_H/\lambda_s)^y, \ \ 0 \le y \le 2 \qquad (6.49)$$

where we have used the inequalities (6.47) in setting the limits on y.

Intuitively, it seems somewhat surprising that we are attributing physical significance to large fields which can become much larger than the limit set by flux quantization through the dominant loop of size $\xi_H(\Phi_0/\xi_H^2)$. Since there is a hierarchy of loops, increasing the field beyond this limit has a real effect and there is no reason to expect that the structure will remain connected up to H_s.

The critical index y requires a better calculation and cannot be determined from the linearized equations we have used. We shall discuss this elsewhere.[16]

D. A lattice of gaskets

Alternatively, one could consider the gasket as a local structure connected into a lattice at some scale. L.[12] We ignore the geometric details and assume that one can use the iterated gasket values (t_n,γ_n) in a lattice model of the type considered in Sec. V. In the scaling regime [Eq. (6.30)] we have

$$\theta_L^2 = 5^n\theta_0^2 = (L/a)^{2+\theta}\theta_0^2 \ , \qquad (6.50)$$

where θ is defined in Eq. (6.40), i.e.,

$$\theta_L^2 \approx (L/\bar{\xi}_s)^2 < 1, \ \ \bar{\xi}_s \approx L^{-\theta/2}\xi_s \ , \qquad (6.51)$$

and using (5.14) with θ_L replacing θ,

$$H_{c2} \propto \Phi_0/\bar{\xi}_s^2 \propto L^{\theta}\Phi_0/\xi_s^2 \ . \qquad (6.52)$$

As in Sec. VI C the renormalized correlation length $\bar{\xi}_s$ cannot become smaller than L. This shows up explicitly through the fact that Eq. (5.6) has no solution when we replace $\cos\theta$ by t_n and $t_n > 1$. [This follows from property (*a*) of the solutions.] Thus condition (6.33) also holds for a lattice. This determines a crossover when L becomes equal to the intrinsic correlation length of the gasket $[\lambda(\xi_s)]$ defined in Eq. (6.41). When L becomes larger we have a situation similar to that we discussed for the finite gasket in Sec. VI C. The critical field is determined by the destruction of loops on the scale L and depends on the properties of the gasket at all smaller scales. Thus setting $\xi_H = L$ in Eq. (6.49),

$$H_{c2}(L) \propto \Phi_0/L^2(L/\lambda_s)^y, \ \ L > \lambda_s \ . \qquad (6.53)$$

The index y cannot be determined from the crossover behavior (at $L = \lambda$).

We have identified the macroscopic critical field of the lattice (as determined, e.g., by the resistive transition) with the field at which loops on the scale L are disrupted. This seems natural and almost inevitable in a scaling model. An explicit calculation demonstrating this would of course be preferable.

An important result is that H_{c2} is a *decreasing* function of L in this regime. The inequality (6.47) requires $y < 2$ in Eq. (6.53). As the field is increased the largest surviving loops become smaller. We shall argue in Sec. VIII that this is a general property of a large class of models for the structure of percolation clusters.

VII. APPLICATION TO THE SSG MODEL

We want to apply these results to percolation clusters taking proper account of their scaling properties and emphasizing the importance of dead ends and loops. In this section we shall discuss predictions for the Skal—Shklovski—deGennes (SSG) model[13] which has dead ends but no loops on a scale smaller than ξ_p. It will be seen that the results are in many ways similar to those we found for the gasket model of Gefen *et al.*[12] Important differences do, however, show up because the field cannot have any effect once coherence is destroyed on the scale ξ_p (there are no loops) and when flux quantization is considered.

A. The bare backbone in the SSG model

For completeness we first consider a bare backbone with no dead ends. We emphasize, however, that the dead ends are crucial for percolation clusters in the linear regime (as they are for the analogous diffusion problem).[14]

One can use the results of Sec. V. One has

$$\gamma \approx 2\pi H\xi_p^2/\Phi_0 \qquad (7.1)$$

in analogy to Eq. (5.4), and

$$\theta = l_p/\xi_s \ , \qquad (7.2)$$

where l_p is the SSG string length[13]

$$l_p \propto (p-p_c)^{-\zeta}, \ \ \zeta = t-(d-2)\nu \ . \qquad (7.3)$$

Thus for small θ one finds, instead of Eq. (5.16),

$$H_{c2} \propto (l_p/\xi_p)^2\Phi_0/\pi\xi_s^2 \ . \qquad (7.4)$$

For large θ,

$$\theta \gtrsim \pi \ , \qquad (7.5)$$

and this behavior breaks down and there is no critical field. Adding a flux quantum per loop has no effect. Another way of formulating this result is to say that the coherence length is reduced by a geometric factor

$$\bar{\xi}_s = (\xi_p/l_p)\xi_s \qquad (7.6)$$

because of the tortuous shape of the one-dimensional links.

For a random system one would expect the Little-Parks oscillations[11] to be damped out and probably some shift in the specific crossover value compared to the lattice result [Eq. (5.20)].

B. The SSG model with dead ends

We have seen that the dead ends are important. Assume first that ξ_s is sufficiently small. One can use the results of Sec. IV C. Setting $d_n = l_p^{-1}$ and $L_n = \xi_p$ in 4.18 gives

$$\bar{\xi}_s \approx \xi_s (\xi_p^2 / l_p m_p)^{1/2} \approx \xi_s (p - p_c)^{(t-\beta)/2} , \tag{7.7}$$

where the mass (m_p) on a scale ξ_p is

$$m_p \propto (p - p_c)^{\beta} \xi_p^d \approx (p - p_c)^{\beta - \nu d} . \tag{7.8}$$

Thus, instead of (7.4) one predicts

$$H_{c2} \propto (\Phi_0 / \pi \xi_s^2)(p - p_c)^{-(t-\beta)} . \tag{7.9}$$

The condition for the validity of this expression is

$$\bar{\xi}_s > \xi_p, \quad \lambda_s \approx \xi_s^{2/(2+\theta)} > \xi_p , \tag{7.10}$$

where[14]

$$\theta = (t - \beta)/\nu . \tag{7.11}$$

This is in reasonably good agreement with the results of Ref. 1 in the small ξ_p (small-resistivity) region. Equation (7.7) is also the result one would obtain if one were to use the infinite cluster diffusion constant $\propto (p - p_c)^{t-\beta}$ (see Refs. 14 , 18, and 23) in the standard expression for $\bar{\xi}_s$.[15]

Consider now the situation close to p_c when (7.10) does not hold. As in Sec. VI C [Eq. (6.41)] we define a length

$$\lambda_s \propto \xi_s^{2/(2+\theta)} \tag{7.12}$$

analogous to the diffusion length.[14] Up to the scale λ_s the renormalized coherence length is always small compared to the relevant l_{ij}. Thus on a scale λ_s one will have

$$m(\lambda_s) \approx \lambda_s^{\bar{d}} \tag{7.13}$$

and

$$l(\lambda_s) \approx \lambda_s^{\zeta/\nu} , \tag{7.14}$$

where the anomalous dimensionality of the cluster is[12]

$$\bar{d} = d - \beta/\nu \tag{7.15}$$

and the length index ζ is defined in Eq. (7.3).

We now try to compute the coherence length on the scale ξ_p in terms of a string of "beads" of size λ_s. The underlying idea is that one has a hierarchy of dead ends.[14] Short dead ends will be incorporated into the backbone mass while long ones (on a scale λ_s) do not matter. In essence, λ_s is the depth to which superconducting coherence is established around the backbone. We are interested in the implications for the propagation of coherence *along* the backbone. We can use the formalism of Sec. IV C. We return to Eqs. (4.11),

$$m(\lambda_s)\Delta_i + [1/l(\lambda_s)](\eta_{i,i-1}\Delta_{i-1} + \eta_{i,i+1}\Delta_{i+1} - 2\Delta_i) = 0 . \tag{7.16}$$

We rewrite this in the form

$$(1/l)(-2t\Delta_i + \eta_{i,i-1}\Delta_{i-1} + \eta_{i,i+1}\Delta_{i+1}) = 0 , \tag{7.17}$$

and use an iterative procedure to eliminate the intermediate (say odd) sites in favor of their neighbors. This is more convenient than an explicit use of Eqs. (4.15).

One finds

$$t_{n+1} = 2t_n^2 - 1 , \tag{7.18a}$$

$$l_{n+1} = 2t_n l_n , \tag{7.18b}$$

and a simple multiplicative relationship for the η. The initial behavior near the $t = 1$ unstable fixed point of (7.18) reproduces the additive solutions we considered in Sec. IV C [e.g., Eq. (4.20)]. Equations (7.18) are, however, very similar to Eq. (6.21). As n increases there is an erratic crossover regime and eventually, for large n one reaches a regime

$$t_{n+1} \approx t_n^2, \quad t_n \gg 1 . \tag{7.19}$$

The coupling between the junction points on the backbone decreases exponentially with L ($=2^n$). We treat this along the same lines as we did in Sec. VI D. We argue that large

$$n_p \approx L / l(\lambda_s) \gg 1 \tag{7.20}$$

implies large t_L and would be inconsistent with long-range order. Since we have already used a similar consistency argument in defining λ_s one is lead to a condition

$$\bar{\xi}_s / \xi_p \approx \lambda_s / \xi_p \approx 1 . \tag{7.21}$$

This should be regarded as a condition on the maximum curvatures consistent with the homogeneous linearized solutions.

As in the discussion of Sec. VI C, $\lambda(\xi_s)$ is the relevant coherence length in the scaling regime (i.e., below ξ_p). Beyond this range amplitude correlations decay exponentially.

One thus predicts two regimes. For small ξ_p,

$$\xi_p < \lambda_s \ , \tag{7.22}$$

and H_{c2} is given by Eq. (7.9). For larger values of ξ_p we can set a lower limit on H_{c2},

$$H_{c2}(\xi_p) \gtrsim \Phi_0/\xi_p^2, \ \ \lambda_s < \xi_p \ , \tag{7.23}$$

from the value of H_{c2} for some *larger* value of ξ_s for which λ would be equal to ξ_p. As in Sec. VI we argue that *decreasing* ξ_s cannot decrease H_{c2}. It is straightforward to justify this with the use of the solutions of the inhomogeneous LG equations in a variational argument along the lines of the argument in Sec. VI D.

Since there are no subsidiary loops there is no analog of the field H_s in this model. A treelike cluster of size λ_s is not affected by a magnetic field.

Having no subsidiary loops also has another consequence. Adding a flux quantum to the flux through a loop cannot have any physical effect. We are thus led back to the results of Sec. V (and VII A) for the square lattice. The critical field cannot be *larger* than ϕ_0/ξ_p^2. Combining this with the lower-limit set in Eq. (7.23) one concludes that there cannot be any true critical field in the SSG model when

$$\lambda_s < \xi_p \ . \tag{7.24}$$

This does not exclude the possibility of important hysteresis effects at higher fields in this model.

The results for finite clusters are analogous. Clusters with no loops are not affected by the field. If the cluster has a single loop (of size L) it can be driven normal by a magnetic field if

$$L \le \lambda_s \ . \tag{7.25}$$

The renormalized coherence length is then given by

$$\bar{\xi}_s \propto L^{-\theta/2}\xi_s \tag{7.26}$$

in analogy to Eq. (7.7), and

$$H_c(L) \propto (\Phi_0/L\bar{\xi}_s) \approx (\Phi_0/\xi_s L^{1-\theta/2}) \ . \tag{7.27}$$

Larger loops should exhibit Little-Parks oscillations.[11] We note that the oscillations should cancel out in a magnetization measurement because of interference effects between loops of different size for large fields. It seems obvious that one needs a better treatment of the loop distribution to get meaningful predictions of critical fields and susceptibilities.

VIII. COMPARISON WITH EXPERIMENT AND IMPLICATIONS FOR THE STRUCTURE OF PERCOLATION CLUSTERS

The formalism we have developed in Sec. II has allowed us to study superconductivity on complex geometrical structures in considerable detail. The results for the weakly disordered regime confirm the intuitive expectations. One finds that the diffusion constant shows up here in the same way it does in dirty superconductors. The renormalization of the coherence length derived in this way also seems to give predictions which are in reasonable agreement with experiment. The explicit derivation from a master equation emphasizes the fact that dead ends are important and that one has to renormalize both the mass and the diffusivity. We believe it is at least conceptually important to emphasize this point. The predictions for this regime follow from general scaling considerations and are not sensitive to the details of the model assumed for the short-range structure. One notes that dead ends are definitely important and the general theorems for fixed amplitude spins are not applicable. (Even for spin systems they do not apply if the strands have a *width* of several spins.)

We have shown that there is a crossover when

$$\xi_p \gtrsim \lambda_s \ , \tag{8.1}$$

where ξ_p is the connectivity length and λ_s is, in essence, the superconducting coherence length in the anomalous short-distance regime. We saw that its relationship to the bare coherence length,

$$\lambda_s \propto \xi_s^{2/(2+\theta)}, \ \ \theta = (t-\beta)/\nu \ , \tag{8.2}$$

follows from general scaling consideration. An equivalent quantity should, therefore, show up also in disordered systems which are not described by a percolation model. Thus one expects a similar crossover behavior near the metal-insulator transition when the electronic localization length becomes large.

As mentioned repeatedly $\lambda(\xi_s)$ is analogous to the finite time diffusion length ($L \propto t^{1/(2+\theta)}$). It is curious to note that the same arguments predict localization of the electronic eigenfunctions

$$L \propto (m\epsilon)^{-1/(2+\theta)} \tag{8.3}$$

with the use of Eq. (3.6). This implies that it would be easier to localize the high-energy states. Since purely geometric disorder of the type we are considering is presumably important in many materials this may be relevant to the understanding of real physical systems. This is of course a local effect, i.e., λ is related to the "mean free path" and not directly to the localization length.

We believe this is an important point for the understanding of properties of disordered systems in situations controlled by the fixed point of the disorder (i.e., for large ξ_p). There are two length scales. The smallest scale which can show up in macroscopic properties is ξ_p. On the other hand, local properties depend on the intrinsic scale λ which can be very short. This can have important effects in suitable experiments. For the effect of magnetic fields on superconductors the important point is that neither ξ_p nor λ_s can be used as a renormalized correlation length in a Landau-Ginzburg equation. There is, therefore, a qualitative difference between the properties of strongly disordered superconductors and that described by such an equation. While λ_s is the correlation length locally, the macroscopic properties predicted depend on the geometrical model and in particular on the distribution of loops. This becomes obvious when one compares the results of the SSG model in Sec. VII with those of a model with a gasketlike backbone related to our analysis in Sec. VI. We shall argue below that one probably requires a considerably more sophisticated model.

We have considered two models for the anomalous structure of percolation clusters. Taking the SSG model literally we found (in Sec. VII) that it should behave like a net with a large mesh when ξ_p becomes sufficiently large. The only length scale is ξ_p and the intrinsic length λ_s only shows up in determining the crossover point. It seems unreasonable to take the model literally in a context where subsidiary loops are obviously important.

For the gasket model we found a "weak-link" behavior due to the interference of the hierarchy of loops. We were also able to set an upper bound on the critical field. This led us to an apparently plausible picture for the behavior of the infinite gasket in a magnetic field. As the field is increased the size of the largest loops that are still continuously superconducting (ξ_H) decreases. We expressed this by a scaling assumption [Eq. (6.48)]. It also leads to the prediction that, beyond the crossover, the critical field should decrease as one approaches the percolation threshold.

It should be emphasized that a proper analysis of the large-gasket situation cannot be carried out in the framework of the linearized Landau-Ginzburg equations. We were therefore not able to calculate the index [Eq. (6.53)] y or even to demonstrate that a gasket actually shows the weak-link behavior described. A proper analysis of this situation will be presented elsewhere.[16] We do, however, believe that the heuristic arguments presented in Sec. VI are convincing.

There is a qualitative disagreement between the predictions we obtained with both models and the experimental results. Deutscher *et al.*[1] find a clear crossover but the critical field still seems to diverge with ξ_p:

$$H_{c2} \propto \xi_p^x , \tag{8.4}$$

where x is a positive number. The experiments also seem quite convincing. This result should be compared with the prediction of Sec. VI, e.g., in the scaling form of Eq. (6.53) with $y<2$. We believe this is a real discrepancy and would like to comment on the implications for the structure of percolation clusters assuming that the analysis of Secs. VI and VII and the experimental results of Ref. 1 are reliable.

In any scaling model H_{c2} must be related to the disruption of loops (of size ξ_p) on the critical infinite cluster at p_c. To fit the experiments one needs a model for which large loops are somehow more stable than small ones.

The gasket model is obviously an oversimplification. There are two obvious corrections. First, one needs dead ends. As we have seen this would change λ_s and the critical indices. The qualitative features of the argument in Sec. VI (for a gasketlike backbone) still hold. The second point concerns the distribution of loops. The gasket has loops on all length scales with probability 1. One would like to replace this by a self-similar statistical distribution for which the probability of forming loops is scale invariant but different from unity.

For a gasket (Fig. 4) this would mean that only a fraction (say, q) of triangles of the size shown are connected at *all* three points *ABC*. Similarily, among triangles of the size *IAC* only this fraction (q) is connected at all three points of type II, III, IV, etc. The probability q must be defined as the loop-forming probability. Among clusters of size L only a fraction q has loops with an area proportional to L^2. Other clusters are treelike on this scale but will in general have smaller loops. The relationship of q to the local probability of forming a junction, say at A, is complex and not relevant here. This leads to a much richer weak-link structure.

Consider first the properties at the scale λ_s which one expects to dominate the properties close to p_c. Since λ_s is still the correlation length, clusters of this size will be driven normal uniformly by a field. There is, however, a distribution of these critical fields presumably dominated by the largest loops in the specific cluster. One guesses

$$p(H)=p(H/H_s) \propto (H_s/H)^l,\ \ l>1,\ H>H_s \tag{8.5}$$

where H_s [$\propto 1/\lambda^2(\xi_s)$] is still defined as in Eq. (6.46). Consider now the implication for larger loops, say of size $L \gg \lambda_s$. The loop will, in general, contain a distribution of "weak links" of size λ_s both for geometric reasons (as in the full-gasket Sec. VI C) and because of the distribution in the critical fields for such regions [$f(H)$—Eq. (8.5)]. The loop will be disrupted when the weakest link becomes normal. Since the critical field is necessarily large (compared to ϕ_0/L^2) this is predominantly a local effect. Supercurrents through large loops are reduced (by flux quantization) and may even be unimportant compared to the effect of the distribution (8.5). One ends up with a probability distribution for disruption of large loops determined by $f(H)$ and by the distribution of regions of size λ_s on the circumference of the loop. The critical field (H_{c2}) is then determined by the requirement that some critical fraction of loops of size ξ_p is disrupted.

Altogether this model seems more realistic than the gasket model. Nevertheless it still predicts a critical field which *decreases* with ξ_p. The probability that a loop of size L has a sufficiently weak link to be disrupted at a field $H(>H_s)$ must *increase* with L in any reasonable model of this type. We believe this reflects the fact that we have started with a fractal geometry with a constant ramification number. For such a geometry large loops are open and renormalize to a ring. This seems to lead to a change, at the crossover which is too dramatic, from a latticelike geometry with a ramification proportional to L^{d-1} on a scale larger than ξ_p to the looplike short-range geometry. One would guess that a fractal short-range structure with a ramification number proportional to some power of L would give a smoother transition and might be consistent with the experimental results. We are, however, not aware of any models which would be suitable for checking this conjecture.

Finally, we would like to comment on the magnetic susceptibility discussed by de Gennes.[3] For the low-field situation below p_c ($H \ll H_L;H_s$) one can neglect the changes in the superconducting amplitude ($|\Delta|$). In this limit the problem is linear. In essence only the size distribution of loops is important, as suggested in Ref. 3, and the problem maps exactly on that of a metallic net in a time-dependent magnetic field. Stephen[24] has recently used this relationship. The susceptibility is dominated by the largest loops. It is important to realize that this completely neglects the effect of supercurrents on the amplitudes.[16] Close to p_c one expects important critical-field effects on the loop distribution, analogous to those which showed up in the discussion of H_{c2}. These should show up in the field dependence of the magnetic susceptibility below p_c (when $\xi_p > \lambda_s$) and also have H_{c2} in the connected regime. Measurements of magnetic field dependence of the susceptibility and specific heat would therefore be of great interest, and should give much more detailed information on the cluster geometry than the low-field measurements.

ACKNOWLEDGMENTS

The author would like to thank G. Deutscher for introducing him to the problems of random superconductors and for much insight. I am grateful to A. Aharoni, O. Entin-Wohlmann, Y. Gefen, H. Gutfreund, R. Orbach, J. Shaham, and M. Weger for many helpful discussions. This work was supported in part by the National Science Foundation under Grant No. DMR-78-10312.

[1](a) G. Deutscher, I. Grave, and S. Alexander, Phys. Rev. Lett. 48, 1497 (1982); (b) G. Deutscher, O. Entin Wohlman, S. Fishman, and Y. Shapira, Phys. Rev. B 21, O. Entin-Wohlman, A. Kapitulnik, and Y. Shapira, *ibid.* 24, 6464 (1981).

[2]P. G. de Gennes, C. R. Acad. Sci. B 292, 279 (1981).

[3]P. G. de Gennes, C. R. Acad. Sci. Ser. B 292, 9 (1981).

[4]G. Deutscher and R. Rosenbaum, Appl. Phys. Lett. 27, 366 (1975); D. V. Gubser and S. A. Wolf, in *Ordering in Two-Dimensions,* edited by S. K. Sinha (North-Holland, Amsterdam, 1980), p. 471.

[5]P. G. Harper, Proc. Phys. Soc. London Sect. A 68, 874 (1955).

[6]M. Y. Azbel, Zh. Eksp. Teor. Fiz. 46, 929 (1964) [Sov. Phys.—JETP 19, 634 (1964)]; Phys. Rev. Lett. 43, 1954 (1979).

[7]A. Rauh, Phys. Status Solidi B 65, K131 (1974); 69, K9 (1975).

[8]W. Y. Hsu and L. M. Falicov, Phys. Rev. B 13, 1595 (1976).

[9]D. R. Hofstadter, Phys. Rev. B 14, 2239 (1976).

[10]S. Aubry and G. Andre, in *Proceedings of the Eighth Colloquium on Group Theoretical Methods in Physics, March 1979,* Vol. 3 of *Annals of the Israel Physical Society,* edited by L. P. Horowitz and Y. Neeman (Hilger and IPC, Bristol, 1980).

[11]W. A. Little and R. Park, Phys. Rev. 133, 97 (1964).

[12]Y. Gefen, A. Aharony, B. B. Mandelbrot and S. Kirkpatrick, Phys. Rev. Lett. 47, 1771 (1981).

[13]A. S. Skal and B. I. Shklovskii, Fiz. Tekh. Poluprovodn. 8, 1586 (1974) [Sov. Phys.—Semicond. 8, 1029 (1975)]; P. G. de Gennes, J. Phys. (Paris) Lett. 37, LI, (1976).

[14]Y. Gefen, A. Aharony, and S. Alexander (unpublished).

[15]P. G. de Gennes, *Superconductivity in Metals and Alloys* (Benjamin, New York, 1977), Chaps. 6 and 7.

[16]S. Alexander and E. Halevi (unpublished).

[17]P. G. de Gennes, Recherches 7, 919 (1976).

[18]M. J. Stephen, Phys. Rev. B 17, 4444 (1978).

[19]M. Weger, S. Alexander, and G. dela Riccia, J. Math. Phys. 14, 259 (1973).

[20]R. Landauer, Philos. Mag. 21, 863 (1970).

[21]P. W. Anderson, D. J. Thouless, E. Abraham, and D. S Fisher, Phys. Rev. B 22, 3519 (1980).

[22]S. Alexander (unpublished).

[23]J. P. Straley, J. Phys. C 13, 2991 (1980).

[24]M. J. Stephen, Phys. Lett. 87A, 67 (1981).